Proceedings of the XXV International School of Semiconducting Compounds, Jaszowiec 1996

NEAR-BAND EDGE SPECTRAL HOLE IN QUANTUM WELL: NO EVIDENCE FOR SUBPICOSECOND PLASMA THERMALIZATION

M. Moško and A. Mošková

Institute of Electrical Engineering, Slovak Academy of Sciences
Dúbravská cesta 9, 842 39 Bratislava, Slovak Republic

We show that at low carrier energies and densities the carriers in a two-dimensional Coulomb gas interact via classical unscreened carrier–carrier collisions. This allows us to calculate exactly the thermalization due to the two-dimensional carrier–carrier collisions in a nonthermal low-density ($\approx 10^{10}$ cm^{-2}) two-dimensional plasma excited near the band edge of an undoped GaAs quantum well. The thermalization is found to be 10–15 times slower than the 200 fs thermalization deduced from the previous spectral-hole burning measurements, which means that the spectral hole does not reflect the thermalization process. We also show that the Born approximation fails in describing such carrier–carrier collisions.

PACS numbers: 73.50.–h, 73.50.Bk, 78.47.+p

A nonthermal two-dimensional (2D) electron–hole (e–h) plasma can be excited in a quantum well (QW) using a quasi-monoenergetic laser pulse of shorter duration than the plasma thermalization time [1–3]. Immediately after the excitation the differential transmission (DT) $DT = N_{\rm w}L_{\rm w}[\alpha_0(\omega)-\alpha(\omega,t)]$ can be probed by a short broad-band pulse. Here α_0 (α) is the absorption of the unexcited (excited) QW, $N_{\rm w}$ — the number of the QWs, $L_{\rm w}$ — the QW width, $\hbar\omega$ — the photon energy, and t — the time delay of the probe pulse. Neglecting coherence effects [4] the band-to-band absorption reads [3] $\alpha(\omega,t) = \alpha_0(\omega)[1 - f_{\rm e}(\varepsilon_{\rm e,t}) - f_{\rm h}(\varepsilon_{\rm h,t})]$, where $f_{\rm e,h}$ is the carrier distribution, $\varepsilon_{\rm e} + \varepsilon_{\rm h} = \hbar\omega - E_{\rm g}$, $\varepsilon_{\rm e,h} = \hbar^2k^2/(2m_{\rm e,h})$ is the carrier energy, $m_{\rm e,h}$ the effective mass, and $E_{\rm g}$ the effective band gap of the QW. Then $DT \propto f_{\rm e}(\varepsilon_{\rm e,t}) + f_{\rm h}(\varepsilon_{\rm h,t})$ and this simple DT model is believed [1–3] to provide experimentally the thermalization of $f_{\rm e} + f_{\rm h}$. The 200 fs thermalization was observed in undoped GaAs QWs [1,2] for the excited e–h pair density $N_{\rm s} \approx 10^{10}$ cm^{-2} and ascribed to 2D carrier–carrier (c–c) scattering assuming the carrier excitation below the optic phonon emission threshold. However, this interpretation has no support in semiclassical Monte Carlo (MC) simulations [5] and molecular dynamics (MD) simulations [5], which give a much slower thermalization. The model $DT \propto f_{\rm e}+f_{\rm h}$ should be tested by comparing the experimental DT

with an exact calculation of the thermalization of $f_e + f_h$. In this paper we succeed in performing such calculation for the low-energy low-density 2D plasma [1,2], since (as we show) the carriers in such plasma interact via classical unscreened 2D c–c collisions.

In Refs. [1,2] electrons and heavy holes were excited into the lowest QW subband. Let us consider classical binary collisions in such plasma. A carrier γ changes its wave vector from $\boldsymbol{k}$ to $\boldsymbol{k}'$ by a collision with a carrier δ, which is scattered from $\boldsymbol{k}_0$ to $\boldsymbol{k}_0'$. The angle Θ between the initial relative wave vector, $\boldsymbol{g} = \mu(\boldsymbol{k}_0/m_\delta - \boldsymbol{k}/m_\gamma)$, and the final one, $\boldsymbol{g}'$, is [6]

$$\Theta = \pi - 2\int_{r_{\min}}^{\infty} \mathrm{d}r \frac{b}{r^2[1-(b/r)^2 - 4V(r)/\mu g]^{1/2}}, \quad \gamma = \mathrm{e,h}, \quad \delta = \mathrm{e,h}, \qquad (1)$$

where b is the impact distance, r — the in-plane distance between the carriers, $r_{\min}$ — the minimum in-plane distance, $\mu = 2m_\gamma m_\delta/(m_\gamma + m_\delta)$, and

$$V(r) = \frac{1}{(2\pi)^2} \int \mathrm{d}\boldsymbol{Q}\, \mathrm{e}^{\mathrm{i}\boldsymbol{Q}\cdot\boldsymbol{r}} \frac{q_\gamma q_\delta}{2KQ} \frac{F_{1111}(Q)}{\varepsilon(Q)}, \qquad (2)$$

where $q_e = -e$, $q_h = e$, K is the material permittivity, $F_{1111}(Q)$ — the form factor [5] and $\varepsilon(Q)$ — the "quasi-dynamic" screening function [5]. For unscreened interaction ($\varepsilon(Q) = 1$) between strictly 2D carriers ($F_{1111}(Q) = 1$) one has $V(r) = q_\gamma q_\delta/4\pi K r$, Eq. (1) gives Rutherford formula $b = (2G/g)\cot(\Theta/2)$ where $G = \mu e^2/4\pi K g\hbar^2$, and equation $\sigma_{\mathrm{cl}} = -\mathrm{d}b/\mathrm{d}\Theta$ gives the differential cross-section $\sigma_{\mathrm{cl}} = G/[g\sin^2(\Theta/2)]$. The same σ_{cl} follows from the exact quantum cross-section $\sigma = G\tanh(\pi G)/[g\sin^2(\Theta/2)]$ [5] for $\pi G \gg 1$, while for $\pi G \ll 1$ one gets the Born approximation $\sigma_{\mathrm{B}} = \pi G^2/[g\sin^2(\Theta/2)]$. Figure 1 shows $\sigma_{\mathrm{B}}/\sigma$ and $\sigma_{\mathrm{cl}}/\sigma$ versus g for the e–e, e–h, and h–h collisions. When g is small, $\sigma_{\mathrm{B}} \gg \sigma$ and $\sigma_{\mathrm{cl}} = \sigma$. Thus,

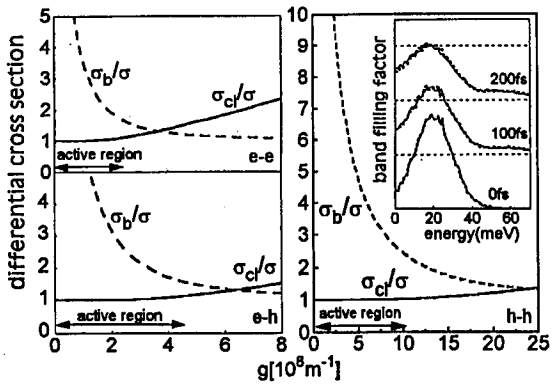

Fig. 1. Unscreened differential cross-section versus g for the e–e, e–h, and h–h collisions. The classical cross-section σ_{cl} and the Born cross-section σ_{B} are compared with the exact quantum cross-section σ. The inset shows the thermalization of the band filling factor $f_e + f_h$ (see the text) for classical c–c collisions with g-values restricted to the "active region" (dotted lines) and with g-values without any restriction (full lines).

if the many-body Coulomb interaction behaves like unscreened classical binary collisions with cross sections $\sigma_{cl} = \sigma$, quantum collisions can be simulated exactly by simulating (via the MC simulation) classical collisions. The collision rate of the carrier γ, colliding with carrier δ, reads

$$\Gamma_{\gamma-\delta}(k) = \sum_{k_0, s_0} f_\delta(k_0) \frac{\hbar g}{\mu} 2b(\Theta = 0, g), \quad \gamma = \mathrm{e,h}, \quad \delta = \mathrm{e,h}, \tag{3}$$

where $2b(\Theta = 0, g)$ is the total collisional cross section and s_0 — the spin of carrier δ. In the MC simulation each carrier in the e–h plasma undergoes stochastic binary collisions according to the collision rates (3). The impact distance b realized in a binary collision of two carriers of wave vector g is selected at random between 0 and $b(\Theta = 0, g)$ and the scattering angle $\Theta = \Theta(b, g)$ is obtained from Eq. (1). This classical MC simulation is similar to the semiclassical one [5], except that the classical rate (3) diverges because Eq. (1) gives $b(\Theta = 0, g) \to \infty$ even for screened $V(r)$. Therefore we replace $b(\Theta = 0, g)$ by a constant finite maximum impact b_{max}, apply the usual MC algorithm [5], and verify that the results do not depend on the choice of b_{max} for large enough b_{max}. We first excite electrons and holes of density $N_s = 2 \times 10^{10}$ cm^{-2} instantaneously into Gaussian energy distributions of widths 17.4 meV and 2.6 meV, centered at energies 17.4 meV and 2.6 meV, respectively [1,3]. The 100 fs duration of the excitation [1] is considered later on. We consider the carrier–optic phonon scattering at 300 K and the c–c collisions due to screened interaction (2).

Using $F_{1111} = 1$ in Eq. (2) we first discuss the case of c–c collisions between strictly 2D carriers. Our classical MC gives the same plasma thermalization for any $b_{max} > d$, where $d = (2N_s)^{-1/2}/2$ is half of the mean interparticle distance. Figure 2a illustrates this finding for $b_{max} = d$ and $b_{max} = 1000d$. Figure 2a also shows the result obtained for unscreened c–c collisions with $b_{max} = d$. The result is the same as for screened c–c collisions with $b_{max} = d$ and $b_{max} = 1000d$, which means that the screening of thermalizing c–c collisions (collisions with $b < d$) is negligible. This allows us to conclude that our classical MC simulates exact quantum c–c collisions, because the unscreened classical and unscreened exact cross sections are the same. Indeed, the inset to Fig. 1 shows that the classical MC gives the same thermalization when only the c–c collisions for g from the "active region" are taken into account. For this region $\sigma_{cl} = \sigma$ to a good precision. Figure 2b shows the semiclassical MC result [5], which treats the c–c collisions in the Born approximation. The thermalization is fast when compared with the exact c–c collisions treatment in Fig. 2a, which is consistent with Fig. 1, where $\sigma_B \gg \sigma$ in the "active region". Full circles in Fig. 2b show the result of the MD simulation [5] of classical many-body Coulomb interactions. The agreement with the MC simulation of classical binary collisions in Fig. 2a proves that the thermalization in the system with many-body Coulomb interactions is governed by unscreened binary collisions with cross sections $\sigma_{cl} = \sigma$. Finally, our classical MC gives the same result as in Fig. 2a, when a realistic form factor is used in Eq. (2) instead of $F_{1111} = 1$. The insensitivity of c–c collisions to the form factor is an important condition of validity of the classical description, because $\sigma_{cl} = \sigma$ (Fig. 1) holds only for $V(r) \propto r^{-1}$. F_{1111} affects $V(r)$ negligibly for $r > L_w = 9.6$ nm. Since in

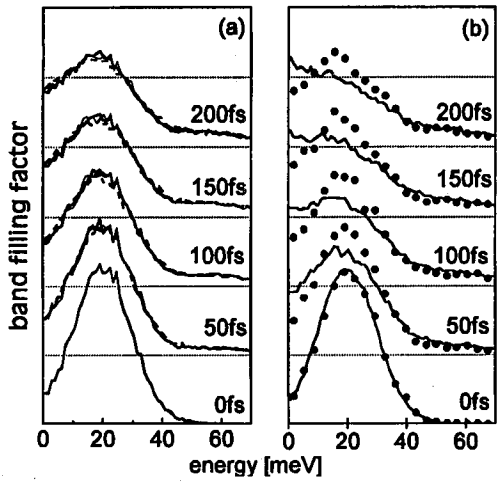

Fig. 2. Band filling factor $f_e + f_h$ versus excess photon energy for times 0,..., 200 fs. Figure (a) shows the results of the MC simulation of screened classical c–c collisions with $b_{max} = d$ (full lines) and $b_{max} = 1000d$ (dashed lines) as well as of unscreened classical c–c collisions with $b_{max} = d$ (thin full lines). Figure (b) shows the semiclassical MC results [5] (full lines) and the classical MD results [5] (full circles). The spacing between the horizontal grid lines is 0.03.

our simulations $r_{min} > 9.6$ nm in most of the c–c collisions, the effect of F_{1111} on scattering angles (1) is negligible.

To compare with experiment [1] we replace the instantaneous excitation by the carrier generation rate $g(k,t) = \int d\omega I(\omega,t)\alpha(\omega,t)L_w/\omega$, where $I(\omega,t)$ is the Gaussian pump spectrum with the central frequency $\hbar\omega_0 = 1509$ meV, the FWHM of 20 meV, and the time duration of 100 fs [1]. We simulate $DT = N_w L_w \alpha_0(\omega) \times (f_e + f_h)$, where $\alpha_0(\omega) = (2.7 \times 10^5\ m^{-1}) \times$ Sommerfeld factor [7]. Figure 3a compares the experimental DT [1] with the DT simulated by our classical MC for $N_s = 2 \times 10^{10}\ cm^{-2}$ and $N_s = 1.1 \times 10^{10}\ cm^{-2}$. The former N_s is the estimation from Ref. [1], but the latter N_s gives a better fit of the spectral hole at 0 fs. In both cases the relaxation of the spectral hole is much slower than in the experiment. Figure 3a also shows that the excess energy $\hbar\omega_0 - E_g = 20$ meV (estimation from Refs. [1, 3]) is too low, because the heavy-hole exciton position of 1457.5 meV and the exciton binding energy of 10 meV [7] give $E_g = 1467.5$ meV and $\hbar\omega_0 - E_g = 41.5$ meV. When $\hbar\omega_0 - E_g = 41.5$ meV, the DT relaxation is faster due to increased optic phonon emission. This is shown in Fig. 3b for $N_s = 1.1 \times 10^{10}\ cm^{-2}$ (thick full lines). When only the c–c collisions are taken into account, we obtain 15 times slower thermalization (dashed lines in Fig. 3b). We conclude that in Ref. [1] the 2D c–c collisions are obscured by phonon emission due to high $\hbar\omega_0 - E_g$. The phonons weakly affect MC results in Fig. 3a. These results are thus more relevant to the experiment of Ref. [2], where $\hbar\omega_0 - E_g \approx 10$ meV. The observed spectral-hole relaxation [2] is much faster than the thermalization in Fig. 3a, i.e., the spectral hole does not reflect the thermalization of $f_e + f_h$, but probably only

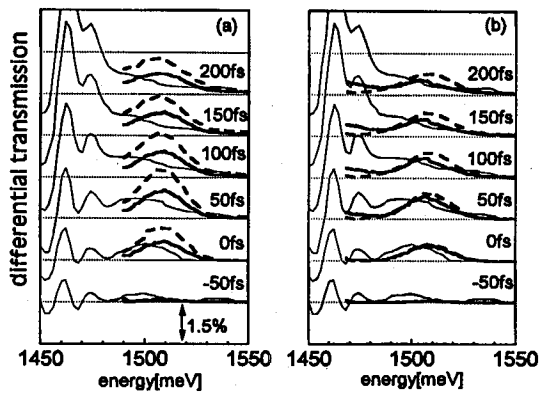

Fig. 3. Differential transmission (DT) versus photon energy. The experimental DT [1] is shown in thin full lines. Figure (a) shows the classical MC results for $N_s = 1.1 \times 10^{10}$ cm^{-2} (full lines) and $N_s = 2 \times 10^{10}$ cm^{-2} (dashed lines). In these calculations $\hbar\omega_0 - E_g =$ 20 meV. Figure (b) shows the classical MC results for $N_s = 1.1 \times 10^{10}$ cm^{-2} with optic phonon scattering omitted (dashed lines) and included (full lines). Here $\hbar\omega_0 - E_g =$ 41.5 meV.

coherence effects. Unfortunately, available theories of coherence effects [4] treat the 3D c–c scattering in the Born approximation, which breaks down in our 2D case (Figs. 1, 2).

References

[1] W.H. Knox, C. Hirliman, D.A.B. Miller, J. Shah, D.S. Chemla, C.V. Shank, *Phys. Rev. Lett.* **56**, 1191 (1986).

[2] J.B. Stark, W.H. Knox, D.S. Chemla, *Phys. Rev. Lett.* **68**, 3080 (1992).

[3] W.H. Knox, in: *Hot Carriers in Semiconductor Nanostructures*, Ed. J. Shah, Academic Press, New York 1992, p. 313.

[4] F. Rossi, S. Haas, T. Kuhn, *Semicond. Sci. Technol.* **9**, 411 (1994).

[5] M. Moško, A. Mošková, V. Cambel, *Phys. Rev. B* **51**, 16860 (1995).

[6] R. Balescu, *Equilibrium and Nonequilibrium Statistical Mechanics*, Wiley, New York 1975.

[7] D.S. Chemla, D.A.B. Miller, P.W. Smith, A.C. Gossard, W. Wiegmann, *IEEE J. Quantum Electron.* **20**, 265 (1984).